Contents lists available at SCCE

Journal of Soft Computing in Civil Engineering

Journal homepage: www.jsoftcivil.com

Modeling the Influence of Environmental Factors on Concrete Evaporation Rate

V.C. Papadimitropoulos[1], P.K. Tsikas[2], A.P. Chassiakos[3*]

1. Ph.D. Candidate, Department of Civil Engineering, University of Patras, Patras, Greece
2. Ph.D., Department of Civil Engineering, University of Patras, Patras, Greece
3. Associate Professor, Department of Civil Engineering, University of Patras, Patras, Greece

Corresponding author: *a.chassiakos@upatras.gr*

https://doi.org/10.22115/SCCE.2020.246071.1254

ARTICLE INFO

Article history:
Received: 31 August 2020
Revised: 12 October 2020
Accepted: 12 October 2020

Keywords:
Concrete evaporation rate;
Plastic shrinkage;
Hot weather concreting;
Artificial neural networks;
Genetic algorithms;
Curve-fitting.

ABSTRACT

Newly poured concrete opposing hot and windy conditions is considerably susceptible to plastic shrinkage cracking. Crack-free concrete structures are essential in ensuring high level of durability and functionality as cracks allow harmful instances or water to penetrate in the concrete resulting in structural damages, e.g. reinforcement corrosion or pressure application on the crack sides due to water freezing effect. Among other factors influencing plastic shrinkage, an important one is the concrete surface humidity evaporation rate. The evaporation rate is currently calculated in practice by using a quite complex Nomograph, a process rather tedious, time consuming and prone to inaccuracies. In response to such limitations, three analytical models for estimating the evaporation rate are developed and evaluated in this paper on the basis of the ACI 305R-10 Nomograph for "Hot Weather Concreting". In this direction, several methods and techniques are employed including curve fitting via Genetic Algorithm optimization and Artificial Neural Networks techniques. The models are developed and tested upon datasets from two different countries and compared to the results of a previous similar study. The outcomes of this study indicate that such models can effectively re-develop the Nomograph output and estimate the concrete evaporation rate with high accuracy compared to typical curve-fitting statistical models or models from the literature. Among the proposed methods, the optimization via Genetic Algorithms, individually applied at each estimation process step, provides the best fitting result.

How to cite this article: Papadimitropoulos VC, Tsikas PK, Chassiakos AP. Modeling the Influence of Environmental Factors on Concrete Evaporation Rate. J Soft Comput Civ Eng 2020;4(4):79–97. https://doi.org/10.22115/SCCE.2020.246071.1254.

1. Introduction

Hot weather can result in several problems throughout the concreting phases (mixing, placing, and curing) and adversely affect concrete properties and its service life. These problems are associated with high concrete temperatures that are primarily caused by fast evaporation of water out of concrete. During evaporation in fresh concrete, three-dimensional volume changes occur mainly due to quick loss of surface bleed water which in turn tends to bring the nearby solid particles closer [1]. Thus, while humidity evaporates over the surface of newly placed concrete more rapidly that it is retained by the bleed water, concrete surface is getting shrunk [2]. Due to that shrinkage, a restraint is triggered by the drying surface layer of the concrete. Therefore, tensile stresses are developed in the feeble, stiffening plastic concrete which in turn produces shallow cracks. These cracks are widespread in almost all directions over the concrete surface and can be sparse or dense [3]. The consequent cracks may occur in either the plastic or hardened state. Accordingly, such developing conditions negatively affect the concrete quality and strength [4].

ACI Committee 305 [5] defines hot weather as any combination of high ambient temperature, high concrete temperature, low relative humidity, high wind velocity and solar radiation. The adverse arrangement of these factors can lead to rapid evaporation of humidity from the fresh concrete surface which, as aforesaid, is the primary cause of plastic shrinkage cracks in concrete. Yet, the analysis by ACI does not include solar radiation as a variable [6]. In principal, fresh concrete is susceptible to plastic shrinkage cracking especially during hot, windy, and dry weather conditions [7].

Plastic shrinkage cracking can seriously affect a concrete member by reducing its durability and strength directly or indirectly [8]. Such occurrence in construction projects can result in substantial repair cost requirement. Hence, a systematic way for controlling this manifestation is essential to prevent such sort of damage from happening, as any impairment that may occur to concrete or concrete members, because of hot weather, can never be fully alleviated [9].

The evaporation rate is a parameter that directly affects concrete plastic shrinkage and further influences the long-lasting, permanency, and strength of concrete structures. As such, the estimation of the evaporation rate is important for any fresh concrete prior to pouring process. The construction industry has been assisted in this direction by the use of an ACI Nomograph c [5] which returns a numerical value of the evaporation rate without describing straightforwardly the sensitivity of evaporation rate in relation to the individual influencing factors. However, the use of the Nomograph is not very workable, especially when multiple estimations are needed within a repetitive type of analysis. Instead, the implementation of mathematical models can highly expedite the process, improve the accuracy, minimize errors in curve reading, and support decision making.

The objective of this work is to develop mathematical models that can be used as efficient alternatives to the Nomograph manual estimation of the water bleeding rate (evaporation rate) over freshly poured concrete surfaces. Alternate methods and development tools are employed, including curve fitting via Genetic Algorithms and Artificial Neural Networks, leading to a

number of models. The models are comparatively tested between each other and with an existing mathematical model from the literature with data coming from two regions, in particular from Country A and Country B. Evaluation results are presented and discussed along with the main conclusions of the study.

2. Background

Concrete plastic shrinkage cracking is usually noticed on beams, slabs, pavements, and, more commonly, on flat concrete surfaces. Several factors can impact cracking due to plastic shrinkage, such as water-cement ratio, aggregate fineness content, member size, admixtures, and on-site practices for pouring the concrete [7]. Concrete shrinkage is one of the key mechanisms leading to the initial crack formation in concrete structures. Concrete shrinks as humidity is diminishing to the environment in addition to self-desiccation that is the moisture depletion through cement hydration process [10]. Yet, the most important reason is the vaporization of water laying on the surface of the freshly poured concrete [11]. Furthermore, evaporation itself is a process leveraged by climatic factors, such as relative humidity, air temperature, temperature of the evaporating surface - namely the concrete surface - and the wind velocity at the surface [5].

According to ACI committee report, the plastic shrinkage cracking is mostly associated with hot weather concreting in dry climates [5]. It arises in unprotected or exposed concrete surfaces, like slabs or pavements, but also happens in beams and footings. In particular, after concrete is poured, settlement of heavier solid particles downwards takes place while free water is forced upwards to the surface where it will finally evaporate. The bleed rate can be directly affected by the parameters of concrete mix, like water to cement ratio, type of cement, amount of fines in the mix, etc., [6]. Cracking phenomena may develop in any climate where the evaporation rate happens to be greater than the rate at which the water surges to the surface by means of bleeding out of the freshly poured concrete.

Plastic shrinkage cracks occur when the surface of the concrete dries rapidly and shrinks before it can gain sufficient tensile strength to resist cracking ([11,12]). The key to prevent plastic shrinkage is to ensure that the evaporation rate does not exceed the bleed rate as this, besides cracking, will lead to additional problems like inadequate hydration [13]. In conclusion, plastic shrinkage cracking rarely happens in hot-humid climates where the relative humidity hardly drops the level of 80% ([5,11]).

Water evaporation from newly set concrete is a complex process depending on several parameters and conditions. Models for estimating the evaporation rate have been investigated for a century now and a development history can be found in [6]. As of now, due to the complexity of the process, the evaporation rate assessment is predominantly done in practice through the use of a Nomograph developed by ACI [5]. The evaporation Nomograph analyzed in ACI 305R-10 is a graph mainly utilized by construction site engineers as a means for estimating the rate of evaporation of surface humidity from concrete, taking into consideration the influence of air temperature, relative humidity, and wind velocity. Nomographs are graphical tools easy to use and visually tempting for estimating some parameters within a usually complex equation [14]. The particular Nomograph (Figure 1) is based on common hydrological methods for valuing the

water evaporation rate from aquatic reservoirs, e.g., lakes, pools, or tanks. Likewise, it is the most accurate means for the estimation of the evaporation rate from a surface that is bleeding water. The evaporation rate value provides an indication of the possible onset of plastic shrinkage cracking [6].

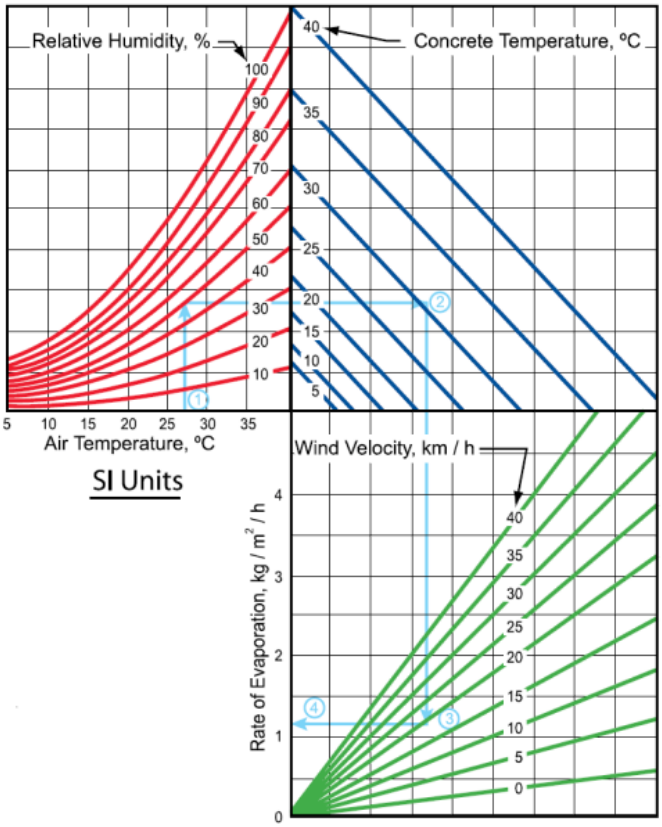

Fig. 1. ACI Nomograph for estimating surface water evaporation rate of concrete. (Source: ACI 305R-10 - Hot Weather Concreting).

Although the Nomograph employment may be quite effective for few or rare estimations in practice, there are certain limitations in its use. First, the estimation is considerably affected by the user subjectivity, especially in the areas where graph lines are quite dense, while there are several intermediate steps until the final result (i.e., the evaporation rate) is obtained. Further, the Nomograph use is rather prone to errors either in reading the correct values or correctly drawing the lines, especially if several calculations are needed. Therefore, some inaccuracies are expected while maneuvering within the graph. Most importantly, the calculations are performed manually, not allowing thus to automate further analyses (and especially those performing iterative processing) that utilize the evaporation rate as an input parameter. Instead, the development of mathematical models can facilitate computational analysis and decision making.

In the direction of developing mathematical relationships, as an alternative to the Nomograph use, Uno has presented a simple formula for estimating the concrete evaporation rate (on the basis of the input parameters of the ACI graph) in the form of the following equation [6]:

$$E = \left(5\left(T_c + 18\right)^{2.5} - r\left(T_a + 18\right)^{2.5}\right)\left(V + 4\right) \times 10^{-6} \quad (1)$$

where:

E = Evaporation rate (kg/m^2/hr),
T_c = Concrete temperature (^{o}C),
T_α = Air temperature (^{o}C),
r = Relative humidity (%),
V = Wind velocity (kph).

Such a formula can serve into some degree the above goals. However, the model simplicity is unavoidably associated with some inaccuracies either in output values or in the application range. For instance, the model effectiveness range is above 15 ^{o}C while the temperature range in the Nomograph starts from 5 ^{o}C. Further, comparison of results provided by the Nomograph and the formula indicates some observable deviations. Considering therefore the current computational capabilities in handling more complex mathematical formulas, if they can provide better estimation results, the present study aims at developing improved mathematical models for estimating concrete evaporation rate that can be further used in concrete work decision making.

3. Methodology

The main scope of this work is to develop mathematical models that can be used for the estimation of fresh concrete evaporation rate as an efficient alternative to the ACI Nomograph use. The latter includes a four-step process indicated by the light blue line in Figure 1. The process starts from the air temperature (X1) and through a clockwise movement, goes through the relative humidity (X3), the concrete temperature (X2), and the wind velocity (X4) leading to the evaporation rate reading (Y) on the lower y axis scale. Among independent parameters, all but (X2) come from meteorological observations. Instead, the concrete temperature (X2) is determined in accordance with the guidelines of ACR 305-10 - Hot Weather Concreting [5] and ACI 207.2R-07 - Report on Thermal and Volume Change Effects on Cracking of Mass Concrete [15] regarding the estimation of the concrete placement temperature in relation to the ambient temperature.

For the model development, a database of meteorological records from two regions in Country A and Country B has been developed. For each data sample, the ACI Nomograph has been manually and carefully employed to estimate the corresponding (target) evaporation rate value (Figure 2). The database is partitioned into three segments to be used for model development (training), validation, and testing respectively. A number of methods and techniques are used to develop mathematical models that best fit the data provided. The developed models are assessed and evaluated upon the validation and testing sets. Several aspects of the validation and testing processes are discussed while the developed models are compared with each other and with the existing model (Equation 1).

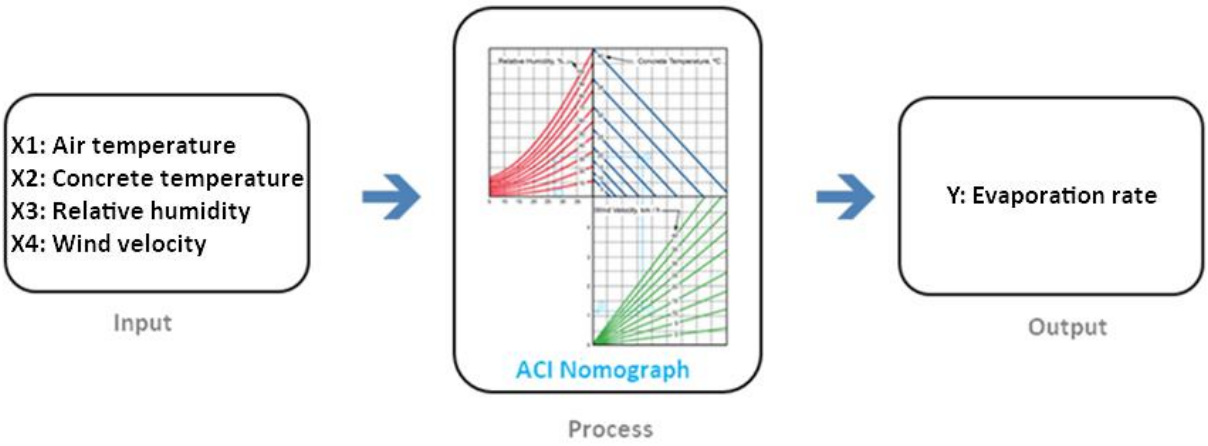

Fig. 2. ACI Nomograph process illustration.

The problem complexity and the non-linear relationships among the involved parameters do not allow a direct identification of a mathematical relation that can estimate the evaporation rate in a trustworthy means. This is because it is necessary to assume a suitable model form that effectively represents the process under analysis. In this regard and in order to examine the possibility of obtaining a solution in terms of a modeling relationship provided by a statistical software, the Stata® software [16] was utilized. The software has been originally developed by StataCorp in 1985 and is primarily engaged to research activities. As it can be seen in the results and discussion section below, such an approach may not be much effective and this calls for more rigorous model development techniques.

In the quest of effective process modeling, optimization methods (e.g., Genetic Algorithms – (GA)) and artificial intelligence methods (Artificial Neural Networks - (NNs)) can be elaborated for optimizing curve-fitting upon input-output datasets. A common strategy is to analyze several types of them - intended to the specific purpose - and compare the degree of fitness to the data provided by means of particular tests. The error between the model estimation and the target value can be minimized through model training. In this study, the statistical Root Mean Square Error (RMSE) is utilized as the main model efficiency assessment parameter. For cross-checking purposes, the (dimensionless) Percent Mean Relative Error (PMRE) parameter is used complimentarily. Finally, for assessing the linearity between estimates and target values, the Correlation Coefficient R and the F-test are employed.

The F-test is a statistical test in which the test statistic has an F-distribution under the null hypothesis. It is mostly used when comparing statistical models that have been fitted to a data set in order to identify the model that best fits the population from which the data were sampled. The customary question in such sort of studies is whether the model estimated values and the real (target) ones are close enough to each other. In response to that query, few perspectives or approaches can be exploited. In this study, it was chosen to rely on a simple test indicating how close the corresponding real and estimated values are scattered around a 45-degree line. Accordingly, a simple regression model of a form

$$y_i = \beta_0 + \beta_1 \circ x_i + \varepsilon_i,\ i = 1,\ldots,n \tag{2}$$

can be utilized for checking the accuracy of the estimation algorithm. Hence, the objective of the analysis is the testing of the following hypothesis [17]:

$$H_0 : \beta_0 = 0 \ \& \ \beta_1 = 1 \ vs \ H_1 : \text{not } H_0 \tag{3}$$

The hypothesis H_0 (or else null hypothesis) can be adeptly checked by means of the F-test where the "general linear hypothesis" is tested.

Regression analysis is a statistical method for identifying the relationships among variables and for making predictions for the output by using mathematical formulas. In case of complex problems and parameter relationships, a common approach for establishing an analytical model based on datasets is the multivariate nonlinear regression. However, the effectiveness of the method largely depends on the degree of the problem non-linearity. Existing statistical software include predetermined types of built-in mathematical relationships (e.g., exponential, logarithmic, polynomial) to be used for curve-fitting. For instance, a typical relationship for associating independent variables ($X_{i=1---n}$) with a dependent variable Y, which is widely exploited by many software applications, is the one shown in Equation 4 (adjusted to the problem under consideration). However, it is not generally feasible to configure tailor-made relationships or to combine different types of relationships within a statistical software so as to potentially improve the accuracy of the outcome.

$$Y = \left(X_1\right)^{a_1} \cdot \left(X_2\right)^{a_2} \cdot \left(X_3\right)^{a_3} \cdot \left(X_4\right)^{a_4} + a_0 \tag{4}$$

In this study, two methods are used to develop approximation models for the evaporation rate estimation. The first performs curve-fitting upon existing data samples by minimizing the root mean square error (RMSE) via Genetic Algorithm (GA) application. Two development approaches are examined. In the first, curve-fitting is straightforwardly performed between input and output values. Because such development does not provide any insight on the interrelationships among the parameters (indicated by the Nomograph) and the corresponding errors within the intermediate steps of the sequential estimation process, an alternative modeling approach is considered by sequentially developing mathematical relationships for each part of the development process. In a different direction, an Artificial Neural Network is alternatively developed to optimally link the input and output parameters of the data set. A short description of the models and the development methodologies are given next.

3.1. Model A1: Global curve-fitting optimized by genetic algorithm

In this development part, a global (single-step) curve-fitting is performed. Following experimentation with alternative non-linear mathematical relationships, a generalization of the nonlinear relationship (4) was finally considered in the form of Equation 5 (Figure 3).

$$Y = A_1 \cdot A_2 \cdot A_3 \cdot A_4 + a_0 \tag{5}$$

$$A_1 = a_{11} \cdot \left(a_{12} \cdot X_1 + a_{13}\right)^{a_{14}} \tag{5-1}$$

$$A_2 = a_{21} \cdot \left(a_{22} \cdot X_2 + a_{23}\right)^{a_{24}} \tag{5-2}$$

$$A_3 = a_{31} \cdot \left(a_{32} \cdot X_3 + a_{33}\right)^{a_{34}} \tag{5-3}$$

$$A_4 = a_{41} \cdot \left(a_{42} \cdot X_4 + a_{43}\right)^{a_{44}} \tag{5-4}$$

where:

Y: Evaporation rate (kg/m^2/hr),
X1: Air temperature (^{o}C),
X2: Concrete temperature (^{o}C),
X3: Relative humidity (%),
X4: Wind velocity (kph).

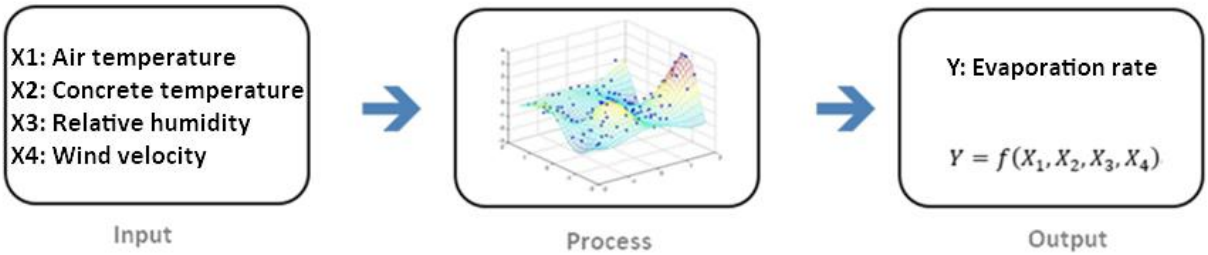

Fig. 3. Model A1 structure: Global curve fitting optimized by Genetic Algorithm.

3.2. Model A2: Step-by-step curve-fitting optimized by Genetic Algorithm

In this development approach, each quadrant of the Nomograph is independently analyzed aiming at assessing and reducing the error associated with the particular part of estimation. The main advantage of this approach is that the whole problem is divided into smaller sub-problems. For each one, a dependent variable is estimated which acts as an independent variable for the next phase. This process makes the whole problem better editable as every sub-problem exerts lower nonlinearity degree. The development structure is indicated in Figure 4 and follows the process being utilized by the Nomograph practice. The result is a set of three mathematical formulas, one for every part of calculations (Equations 6.1-6.3) corresponding to the Nomograph associated quadrants. The formula types were derived after experimentation with alternative mathematical forms.

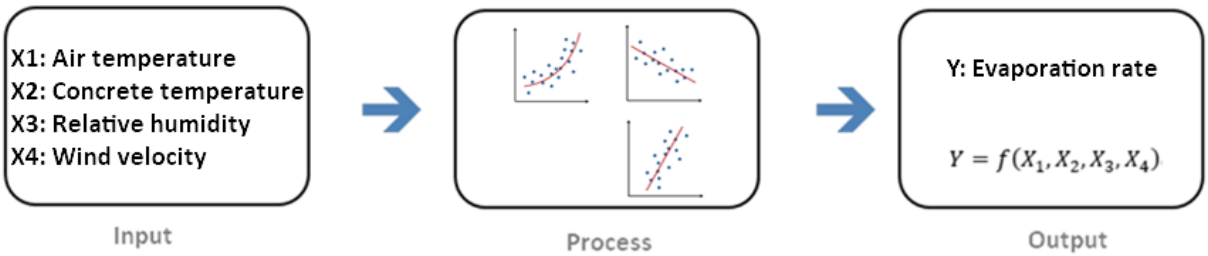

Fig. 4. Model A2 structure: Step-by-step parameter modeling optimized by Genetic Algorithm.

$$Y_1 = b_{11} \cdot e^{b_{12} \cdot X_1} + b_{13} \cdot \left(\left(b_{14} - X_3\right) \cdot \left(b_{15} \cdot X_1 - b_{16}\right)^{b_{17}}\right) + b_{18} \tag{6-1}$$

$$Y_2 = b_{21} \cdot Y_1 + b_{22} \cdot \left(b_{23} - Y_1\right) \cdot \left(b_{24} \cdot X_2 - b_{25}\right)^{b_{26}} + b_{27} \tag{6-2}$$

$$Y = b_{31} \cdot Y_2 + b_{32} \cdot \left(b_{33} - Y_2\right) \cdot \left(b_{34} \cdot X_4 - b_{35}\right) + b_{36} \tag{6-3}$$

where:

Y: Evaporation rate (kg/m^2/hr),
X1: Air temperature (^{o}C),
X2: Concrete temperature (^{o}C),
X3: Relative humidity (%),
X4: Wind velocity (kph).

In both models, A1 and A2, genetic algorithms (GA) were employed to minimize the error between input and output values. A genetic algorithm is a metaheuristic inspired by the natural process of evolution and rather constitutes the basis for evolutionary algorithms development. Genetic algorithms utilize an initial random population of applicable solutions with individuals representing distinct problem solutions and progressively move towards better solutions on the ground of previous solutions. In particular, new solutions evolve iteratively from the current population by stochastically selecting individuals and performing actions like recombination (crossover) or characteristic modification (mutation) to develop offspring which are accepted or not depending on their degree of fitness (optimization value). As with all types of evolutionary algorithms, genetic algorithms do not guarantee full convergence to the optimal solution in any case; yet they have been found capable of closely approaching it in several problems and at a reasonable computational time.

3.3. Model B: Neural network model development

An alternative approach for modeling the evaporation rate estimation process is through the development of an artificial neural network (ANN). In principal, there are several types of ANNs which differ in architecture, the way they calculate the signals in each neuron, and the training algorithm. The main types include the Multi-Layer Feedforward (MLF), the Generalized Regression Neural (GRN) and the Probabilistic Neural (PN) ANN. The main advantages of the GRN/PN types are that they do not require setting topology specifications (e.g., number of hidden layers and nodes) and their training can be fast. Yet, their drawback is that they may not be as reliable for predictions (estimations) and classifications as the MLF type which, on the contrary, requires topology specifications by the developer and presents longer training time. The MLF type uses the back-propagation (BP) algorithm [18] for calculating the aggregate values during training.

For the problem under analysis, the simulation was carried out by a MLF type for improving the accuracy level in estimations. The MLF type acts as a “universal” approximator [19] and can practically simulate any form of complex function with its efficiency being mainly determined by the appropriate selection of the network parameters, i.e., number of nodes and hidden layers, activation function, and learning algorithm. The ANN employed in this study consists of four input neurons (representing the input variables), two hidden layers with four neurons each and an

output neuron for the result (Figure 5). The selection of this structure follows existing knowledge indicating that the use of two layers can efficiently solve several problems of such kinds ([20,21]) while a larger number of neurons can lead to unnecessarily prolonged learning times. The sigmoid function is used as the neuron activation function (transfer function). This is the most commonly used function in ANN development as it is continuous, differentiable, and can vary within any desirable value range. The training goal is to determine the neural network weights so that the Root Mean Square Error (RMSE) parameter is minimized.

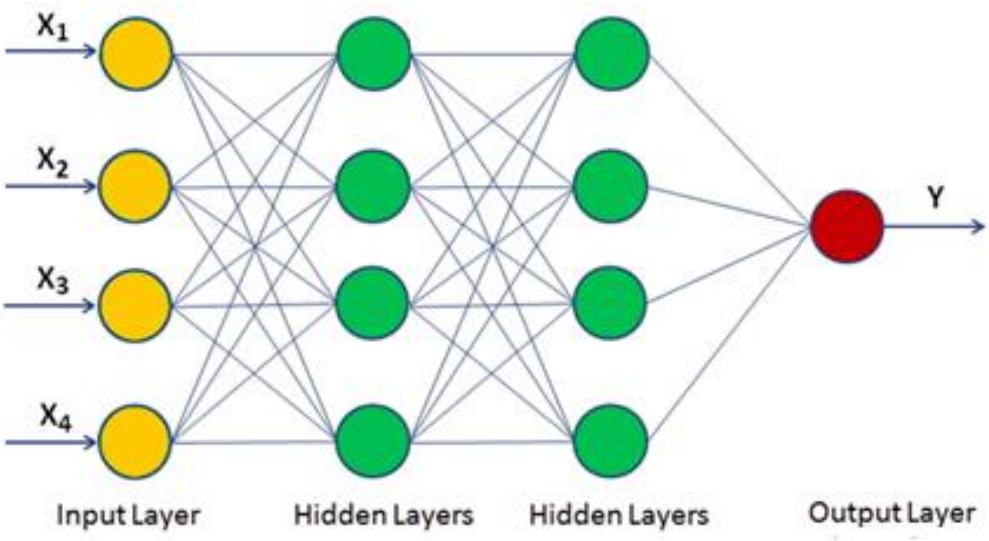

Fig. 5. Neural network structure for Model B.

3.4. Statistical model Stata

The alternative of employing existing statistical software and its capability in developing regression models for curve-fitting is explored in addition. The fractional polynomials option of the Stata® software was used to obtain the parameterization equation. Fractional polynomials are an alternative to regular polynomials that provide flexible parameterization for continuous variables [22]. Following input and output data insertion, the fractional polynomials application returned the following formula:

$$Y = 0.0342\left(\left(\frac{X_1}{10}\right)^3 - 10.2428\right) - 0.0219\left(X_2 - 24.1672\right) - 0.0087\left(X_3 - 65.9310\right) + 0.2149\left(\left(\frac{X_4}{10}\right)^2 - 1.1647\right) - 0.0470\left(\left(\frac{X_4}{10}\right)^3 - 1.2570\right) + 0.3681 \quad (7)$$

where:

Y: Evaporation rate (kg/m^2/hr),
X1: Air temperature (^{o}C),
X2: Concrete temperature (^{o}C),
X3: Relative humidity (%),
X4: Wind velocity (kph).

4. Data management and development software

The problem of concrete dehydration and shrinkage cracking is more exaggerated in warm climates. Therefore, data from such areas were targeted for the model development. On the other hand, the models should be able to function with comparable accuracy within the full allowable concreting temperature range. In this regards, data from two different areas (City A, Country A and City B, Country B) and time periods (2018 and 2019) where used for model development and testing. Both places envisage meteorological conditions that reasonably fit to the desirable parameter ranges including the important hot weather conditions in summer. Meteorological data were then extracted from two year records with random sampling at every 10-day period (four samples per period) of each calendar month ensuring a rather uniform data sampling for impartiality purposes.

Tables 1 and 2 present some indicative snapshots of the meteorological data from the two areas, as they have been organized into Microsoft Excel™ sheets for further processing. Each city sample includes 144 recordings (12 per month). Out of the 288 data sets, 50 percent was used for model training, 25 percent for validation and another 25 percent for testing. According to Green [23], the sample set size for training in such type of analyses should be above an approximate level of fifty plus four times the number of independent parameters, i.e., 82 samples in this development case. The training data set here includes 144 samples and this is well above the proposed threshold.

Table 1
Input data from the City A, Country A.

No	Month	Day	Air temp (^{o}C)	Relative humidity (%)	Wind velocity (kph)
1	Jan	2	9.7	54.0	29.2
2	Jan	9	7.2	63.6	4.0
3	Feb	13	11.7	53.2	12.2
4	Feb	28	13.3	85.8	9.5
5	Mar	24	15.8	77.1	30.2
6	Mar	26	17.0	78.3	33.4
7	Apr	20	16.8	77.4	15.1
8	Apr	30	18.1	82.7	18.5
9	May	7	23.2	72.9	14.1
10	May	27	19.7	84.5	13.9
11	Jun	3	27.8	49.3	19.3
12	Jun	25	24.4	81.4	13.3
13	Jul	22	36.2	39.3	23.9
14	Jul	29	29.0	82.9	8.6
15	Aug	8	33.1	43.9	23.4
16	Aug	24	27.6	72.3	15.1
17	Sep	7	28.0	81.2	13.6
18	Sep	20	25.3	80.4	6.5
19	Oct	19	23.9	72.2	21.6
20	Oct	30	18.8	50.9	2.8
21	Nov	4	22.0	38.7	5.3
22	Nov	7	18.1	53.0	6.4
23	Dec	3	19.0	53.8	14.8
24	Dec	30	13.9	70.8	4.3

Table 2
Input data from the City B, Country B.

No	Month	Day	Air temp (°C)	Relative humidity (%)	Wind velocity (kph)
1	Jan	23	7.0	93.0	4.0
2	Jan	23	11.0	77.0	2.0
3	Feb	4	13.0	63.0	2.0
4	Feb	13	15.0	68.0	13.0
5	Mar	19	33.0	12.0	15.0
6	Mar	24	18.0	88.0	24.0
7	Apr	4	15.0	77.0	4.0
8	Apr	30	32.0	21.0	11.0
9	May	20	32.0	43.0	11.0
10	May	27	23.0	74.0	7.0
11	Jun	3	27.0	58.0	17.0
12	Jun	15	31.0	31.0	11.0
13	Jul	5	32.0	59.0	20.0
14	Jul	22	27.0	70.0	11.0
15	Aug	8	27.0	74.0	9.0
16	Aug	24	32.0	52.0	15.0
17	Sep	7	26.0	70.0	13.0
18	Sep	20	31.0	43.0	17.0
19	Oct	8	23.0	74.0	6.0
20	Oct	24	32.0	36.0	11.0
21	Nov	1	30.0	11.0	20.0
22	Nov	22	19.0	64.0	6.0
23	Dec	3	24.0	41.0	13.0
24	Dec	30	15.0	77.0	19.0

The sampling was organized in a random basis so as to prevent any bias or interrelations among pieces of data and allow likewise every single recording the same chance for being selected. In addition, a wide range of parameter values have been represented in the dataset. In particular, the ambient temperature values are in the range of 7 °C to 38.7 °C, the relative humidity values between 11% and 94%, and the wind velocity values from 1 kph to 39 kph.

Genetic algorithm implementation for models A1 and A2 was performed through the Palisade Evolver™ software which runs as a Microsoft Excel™ add-in. The parameter to be optimized is the Root Mean Square Error (RMSE) between input and output values. In terms of the genetic algorithm parameters, the population size was set at 50 chromosomes, the crossover rate at 50%, and the mutation rate at 10%.

Neural network development was done through the Palisade NeuralTools™ application which also runs as a Microsoft Excel™ add-in. The NeuralTools™ application supports all aforementioned types of ANNs, among which the MLF (Multi-Layer Feedforward) type that was employed in this study. The backpropagation algorithm was used for the ANN training with the the goal to calculate the synaptic weights by minimizing the Root Mean Square Error (RMSE) within the training sample.

5. Results and discussion

In this section, the results of model calibration and validation are presented with appropriate comparisons regarding model efficiency and accuracy. The model coefficients for cases A1 and A2, as developed through the training dataset, are presented in Tables 3 and 4 respectively.

Table 3
Model A1 coefficients.

a_{ij}	1	2	3	4
0	- 0.07780			
1	2.23559	3.66167	11.02054	5.24413
2	11.50336	3.68125	-17.57696	-2.77908
3	12.48055	0.15160	7.44044	-1.59311
4	6.07940	-1.24607	118.71189	-3.35225

Table 4
Model A2 coefficients.

b_{ij}	1	2	3	4	5	6	7	8
1	15.23160	0.04253	-0.00022	70.47599	1.8	-15.62668	1.87571	-1.53674
2	-1.08108	-0.00043	-250	1.8	7.31097	1.55541	62.79499	
3	-0.01180	-0.00241	40.00078	0.62137	-7.44470	0.47220		

For evaluating the efficiency of the developed models and accuracy of results, several forms of graphical result representations and numerical indicators are used. Figures 6-8 show the regression results between the estimated and measured values resulting from the proposed models and in relation to the three datasets (training, validation, and testing) respectively. In addition, a similar analysis and results are presented with regard to the existing Uno model of Equation (1). Figure 9 presents the output of the Stata® software with respect to the deviations between the actual and estimated values of the evaporation rate in each of the three analysis datasets. Finally, Table 5 summarizes the statistical results and efficiency measures of each model in the analysis.

The results indicate that there is a tolerable performance of all models in terms of the Root Mean Square Error and the Percent Mean Relative Error. Among all, models A2 and B present noticeably higher fitting performance in comparison to other models in terms of the above performance parameters and the correlation coefficint R, the latter indicating a strong linearity between estimated and actual values (Table 5). Further, there exists a strong approximation of the ideal line y=x between estimated and actual values in all models but Uno's one, as is indicated by the approximation lines shown in Figures 6-8. In particular, while the x coefficient in models A1, A2 and B are very close to 1.0, the same coefficient in Uno's model is about 0.9 indicating a global underestimation of the expected evaporation rate value within the entire analysis range. This is also indicated by the F-Test results in Table 5 which shows that the null hypothesis is rejected. The Stata model presents widerly scattered approximation points in comparison to other

methods (as also presumed by the R values in Table 5) and a noticable deviation from the 45 degree line between model output and target values. This deviation is, however, smaller than that of Uno's model results.

The following conclusions can be further drawn from the analysis. Comparing the results between models A1 and A2 indicates that in a complex and segmented process, it is more effective to model each segment individually (if feasible) rather than to consider the entire process as a whole. In the former case, there is more effcient handling of individual errors within each step. Further, the result comparison between models A1 and B indicates that an ANN may be more capable to develop a robust model to simulate a complex process than a curve-fitting process which is hampered by the need to assume a proper mathematical formula type. Finally, the comparison among A1, B, and Uno's model reveals the trade-off between model simplicity and expected estimation accuracy. In fact, Uno's model is simpler than the ones developed in this study and this is its main advantage. On the other hand, with currently available computational power and in the aim of obtaining more accurate results that facilitate subsequent concrete analyses, the use of somewhat more complex formulas does not observably burdens the computational effort while improving accuracy. Figure 10 indicatively illustrates the convergence chart of the Genetic Algorithm in the case of Model A1. It can be seen that there is a fast and strong initial convergence of the objective parameter value (RMSE) followed by a longer computational process with much slower convergence rate towards the minimum value.

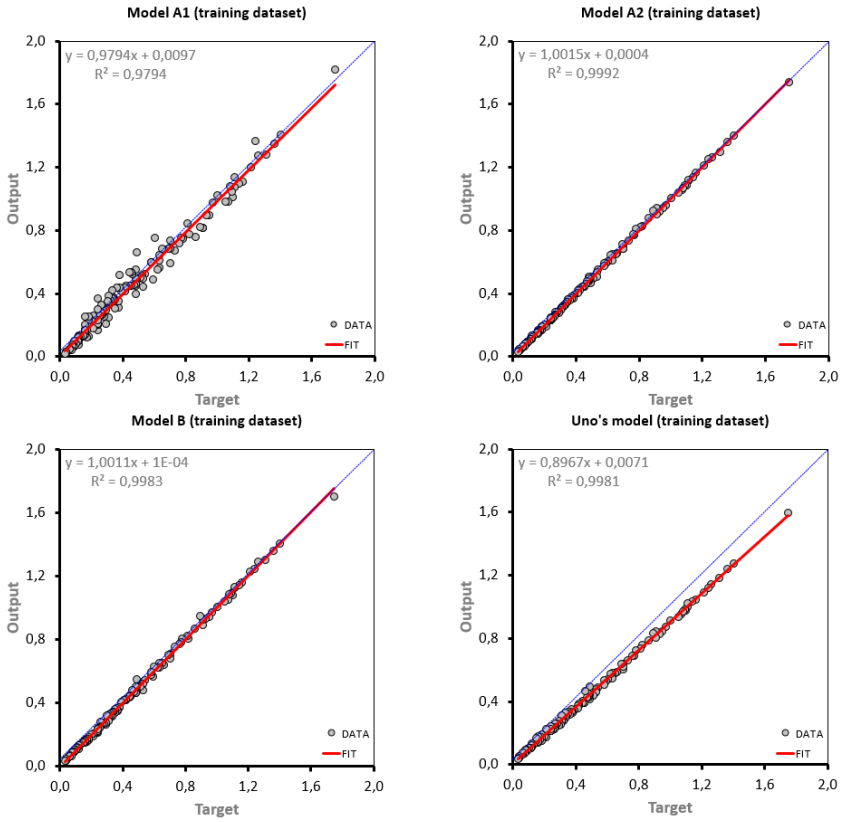

Fig. 6. Modeling results for the training dataset.

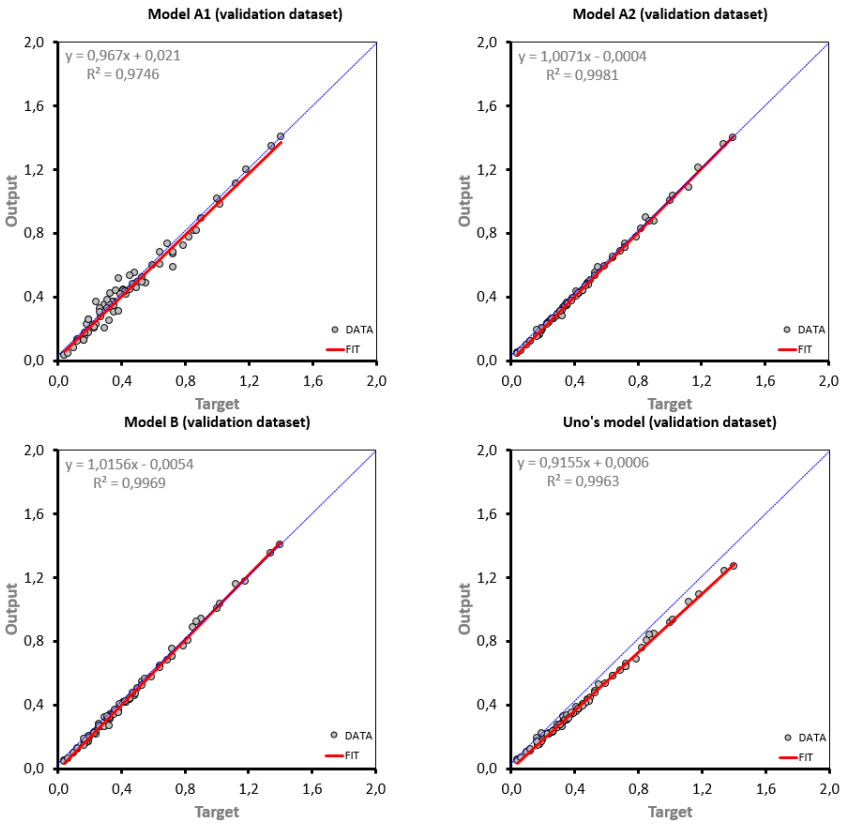

Fig. 7. Modeling results for the validation dataset.

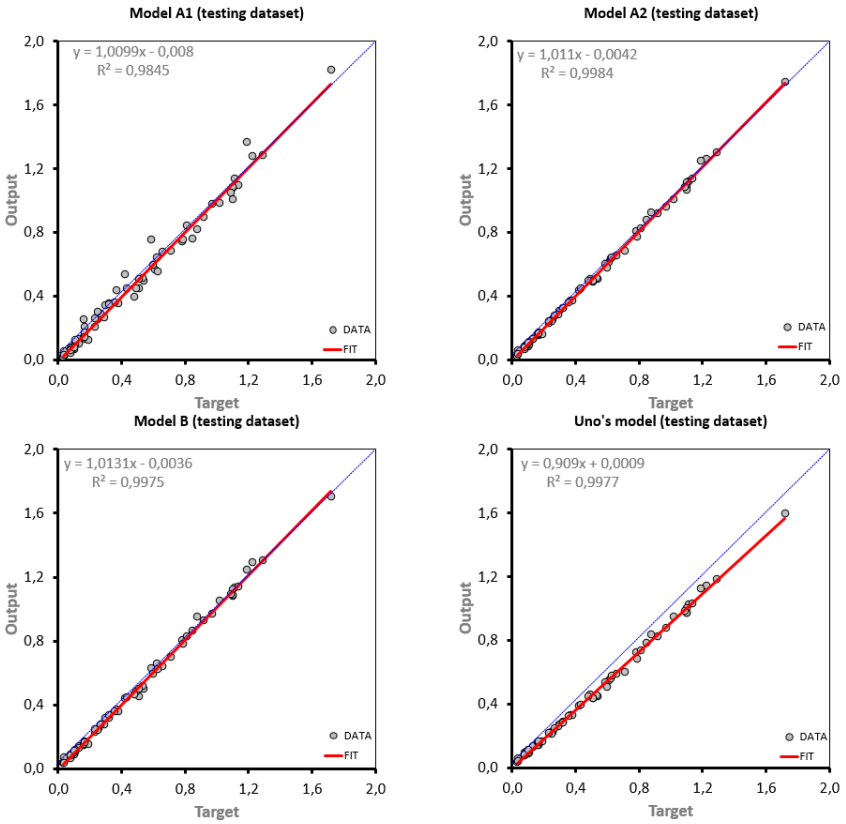

Fig. 8. Modeling results for the testing dataset

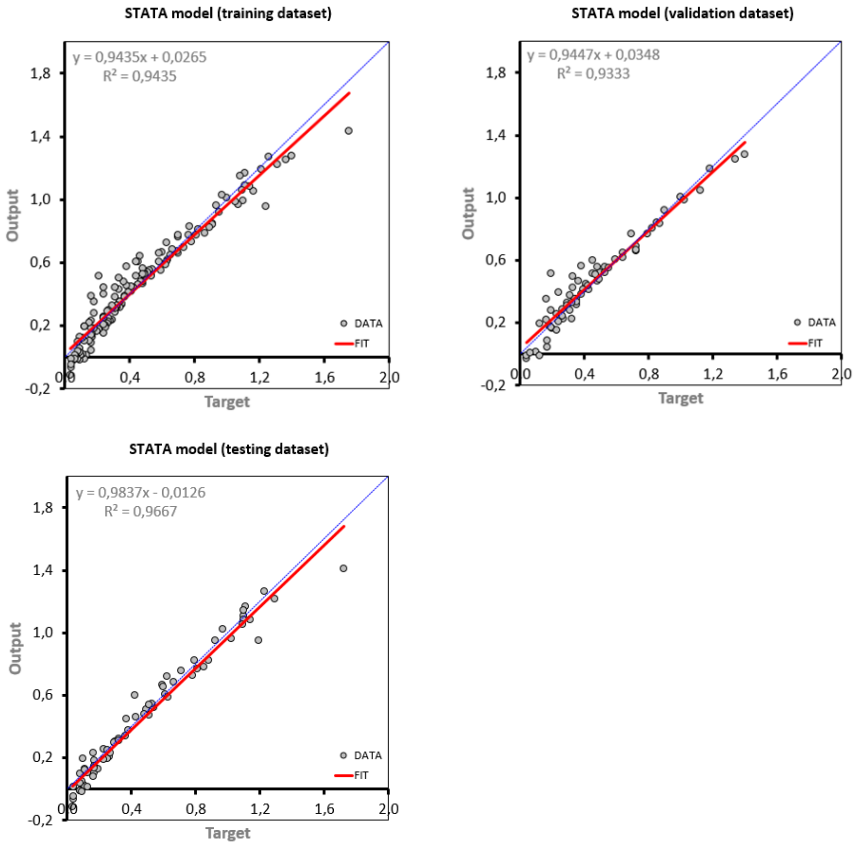

Fig. 9. Stata model results

Table 5
Statistical indicators for all models.

Model	Root mean square error (RMSE)	Percent mean relative error (PMRE)	Correlation coefficient (R)	F-Test*
Training dataset				
Model A1	0.0509	12.18%	0.9896	1.49
Model A2	0.0100	2.29%	0.9996	1.12
Model B	0.0148	3.59%	0.9991	0.17
Uno model	0.0570	9.22%	0.9990	1108.00
STATA	0.0843	30.81%	0.9713	1.49
Validation dataset				
Model A1	0.0489	11.77%	0.9872	2.05
Model A2	0.0139	3.01%	0.9990	2.42
Model B	0.0178	4.50%	0.9985	2.95
Uno model	0.0488	10.39%	0.9981	244.45
STATA	0.0793	25.40%	0.9661	2.16
Testing dataset				
Model A1	0.0503	12.74%	0.9922	0.35
Model A2	0.0167	4.05%	0.9992	2.65
Model B	0.0209	5.46%	0.9987	2.92
Uno model	0.0587	10.01%	0.9988	359.58
STATA	0.0753	34.53%	0.9832	3.00

*Critical value $F_{2,\ 142,\ 0.05} = 3.07$ for training dataset | $F_{2,\ 70,\ 0.05} = 3.13$ for validation & testing datasets.

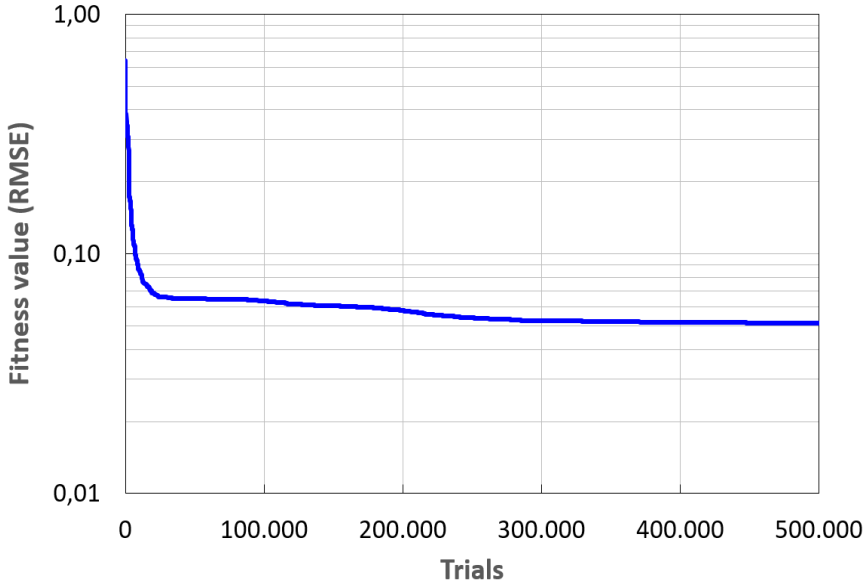

Fig. 10. Genetic Algorithm convergence chart for Model A1.

6. Conclusions

The preservation of newly poured concrete in hot and windy conditions from fast dehydration is considerably important in safeguarding concrete from plastic shrinkage cracking. Among other factors influencing plastic shrinkage, an important one is the concrete surface humidity evaporation rate. The evaporation rate is currently calculated in practice by the use of the ACI 305R-10 Nomograph for "Hot Weather Concreting", a process rather tedious, non-automated, time consuming and prone to errors. In response to such limitations, analytical models for estimating the evaporation rate are developed and evaluated in this work. The development utilizes techniques like optimal curve-fitting via Genetic Algorithm optimization and Artificial Neural Networks.

Based on meteorological data from two different areas, three models have been developed. The first two perform curve-fitting via Genetic Algorithm optimization, either considering the full process as a whole (model A1) or examining each process segment separately and assembling results (model A2). The third model is developed upon an Artificial Neural Network which simulates the entire estimation process (model B). In each case, wide experimentation was performed to fine-tune the model characteristics. For developing a better understanding of the proposed model performance, a typical curve-fitting method through the employment of a statistical software as well as an existing model from the literature were also examined in the analysis.

Evaluation results indicate that the proposed models can effectively assess the proper values of the evaporation rate over the entire range of the independent parameters. Among them, models A2 (step-by-step curve fitting) and B (artificial neural network) present the best performance in terms of the statistical error indicators between estimated and actual values. Further, result

comparisons with the statistical software output and with the existing simple mathematical model from the literature reveal that the proposed models, being more comprehensive, exert higher accuracy and this outcome can be explained by the non-linearity and complexity of the actual estimation process.

Funding

This research received no external funding.

Conflicts of Interest

The authors declare no conflict of interest.

References

[1] Sivakumar A, Santhanam M. A quantitative study on the plastic shrinkage cracking in high strength hybrid fibre reinforced concrete. Cem Concr Compos 2007;29:575–81. doi:10.1016/j.cemconcomp.2007.03.005.

[2] Wittmann FH. On the action of capillary pressure in fresh concrete. Cem Concr Res 1976;6:49–56. doi:10.1016/0008-8846(76)90050-8.

[3] El-Reedy M. Onshore Structural Design Calculations: 9.2.1 Plastic Shrinkage Cracking.Elsevier Ltd. 2017:387–430.

[4] https://assets.master-builders-solutions.basf.com/en-us/hot%20weather%20concreting %20ctif.pdf, last assessed: 27.02.2020. n.d.

[5] ACI Committee 305. Hot-Weather Concreting. ACI 305R-10, American Concrete Institute 2010.

[6] Uno PJ. Plastic shrinkage cracking and evaporation formulas. ACI Mater J 1998;95:365–75.

[7] Sayahi F, Emborg M, Hedlund H. Plastic shrinkage cracking in concrete: State of the art. Nord Concr Res 2014;51:95–110.

[8] Grzybowski M, Shah SP. Shrinkage cracking of fiber reinforced concrete. Mater J 1990;87:138–48.

[9] Mouret M, Bascoul A, Escadeillas G. Strength impairment of concrete mixed in hot weather: relation to porosity of bulk fresh concrete paste and maturity. Mag Concr Res 2003;55:215–23. doi:10.1680/macr.2003.55.3.215.

[10] Zhang J, Hou D, Han Y. Micromechanical modeling on autogenous and drying shrinkages of concrete. Constr Build Mater 2012;29:230–40. doi:10.1016/j.conbuildmat.2011.09.022.

[11] Al-Fadhala M, Hover KC. Rapid evaporation from freshly cast concrete and the Gulf environment. Constr Build Mater 2001;15:1–7. doi:10.1016/S0950-0618(00)00064-7.

[12] Schmidt M, Slowik V. Instrumentation for optimizing concrete curing. Concr Int 2013;35:60–4.

[13] Boshoff WP, Combrinck R. Modelling the severity of plastic shrinkage cracking in concrete. Cem Concr Res 2013;48:34–9. doi:10.1016/j.cemconres.2013.02.003.

[14] Douglas J, Danciu L. Nomogram to help explain probabilistic seismic hazard. J Seismol 2020;24:221–8. doi:10.1007/s10950-019-09885-4.

[15] ACI Committee 207.2R-07. Report on Thermal and Volume Change Effects on Cracking of Mass Concrete, American Concrete Institute, 2007 n.d.

[16] Why Stata, https://www.stata.com/why-use-stata/, last assessed: 01.08.2020 n.d.

[17] Economou P, Batsidis A, Kounetas K. Evaluation of the OECD's prediction algorithm for the annual GDP growth rate. Commun Stat Case Stud Data Anal Appl 2020:1–21. doi:10.1080/23737484.2020.1805818.

[18] Sharifi Y, Hosainpoor M. A Predictive Model Based ANN for Compressive Strength Assessment of the Mortars Containing Metakaolin. J Soft Comput Civ Eng 2020;4:1–12.

[19] Hornik K, Stinchcombe M, White H. Multilayer feedforward networks are universal approximators. Neural Networks 1989;2:359–66. doi:10.1016/0893-6080(89)90020-8.

[20] Esmailzadeh A, Kamali A, Shahriar K, Mikaeil R. Connectivity and Flowrate Estimation of Discrete Fracture Network Using Artificial Neural Network. J Soft Comput Civ Eng 2018;2:13–26.

[21] Luo X, Patton AD, Singh C. Real power transfer capability calculations using multi-layer feed-forward neural networks. IEEE Trans Power Syst 2000;15:903–8. doi:10.1109/59.867192.

[22] Fractional Polynomial Regression, Chapter 382, https://ncss-wpengine.netdna-ssl.com/wp-content/themes/ncss/pdf/Procedures/NCSS/Fractional_Polynomial_Regression.pdf, last assessed: 01.08.2020. n.d.

[23] Green SB. How Many Subjects Does It Take To Do A Regression Analysis. Multivariate Behav Res 1991;26:499–510. doi:10.1207/s15327906mbr2603_7.